Fast reconstruction of an unmanned engineering vehicle and its application to carrying rocket

Jun Qian, Huabing Zhu, Shuwang Wang, Yishan Zeng

School of Mechanical and Automotive Engineering, Hefei University of Technology, 193 Tunxi Road, Hefei 230009, Anhui Province, People's Republic of China
E-mail: hfuthbzhu@163.com

Published in *The Journal of Engineering*; Received on 26th October 2013; Accepted on 26th February 2014

Abstract: Engineering vehicle is widely used as a huge moving platform for transporting heavy goods. However, traditional human operations have a great influence on the steady movement of the vehicle. In this Letter, a fast reconstruction process of an unmanned engineering vehicle is carried out. By adding a higher-level controller and two two-dimensional laser scanners on the moving platform, the vehicle could perceive the surrounding environment and locate its pose according to extended Kalman filter. Then, a closed-loop control system is formed by communicating with the on-board lower-level controller. To verify the performance of automatic control system, the unmanned vehicle is automatically navigated when carrying a rocket towards a launcher in a launch site. The experimental results show that the vehicle could align with the launcher smoothly and safely within a small lateral deviation of 1 cm. This fast reconstruction presents an efficient way of rebuilding low-cost unmanned special vehicles and other automatic moving platforms.

1 Introduction

Unmanned moving platforms use intelligent control systems to take the place of human beings for exploration in various environments, including ground, aerial and underwater situations. In this big family, intelligent vehicle [1] has attracted huge research interest thanks to its automatic driving and its value in intelligent transportation system. To ensure safety, intelligent vehicle integrates on-board sensors to detect the surrounding environment and estimate its position absolutely and relatively. For example, global positioning system (GPS) is a typical travel assistance device for outdoor mobile platform [2]. Meanwhile, sensors using relative measurement techniques are applied widely in order to acquire environmental data, for example, laser scanner and camera [3]. These sensors could detect static objects, moving pedestrians and border of roads to increase driving safety [4, 5].

Furthermore, the technology of intelligent vehicle could be extended to the fields of construction equipment for the sake of higher efficiency and more extensive application areas than the traditional machines under manual operations, and the development of construction robots and other automated engineering equipments [6]. Ha *et al.* [7] used a two-level control system to build a robotic excavator so as to plan and execute the excavation task automatically. Yamamoto *et al.* [8] integrated several exteroceptive sensors to perceive the surrounding environment for automatic excavation, which needed too much cost. Marshall *et al.* [9] presented a trial load-haul-dump machine for underground mining automation, which mainly measures the external force acting on the mechanism. Lu *et al.* [10] presented a positioning system for construction vehicle with GPS and other new communication tools, but this system needs the job site to be specifically arranged before working. According to the current research, it is necessary to find a universal method to change an existing engineering equipment to an automated one with low-cost and high convenience.

This paper will present a fast reconstruction process of an unmanned engineering vehicle, which is based on a traditional flat-bed truck. The rest of this paper is organised as follows. Section 2 describes the process of fast reconstruction on the basis of an engineering vehicle. Section 3 presents the positioning system for carrying rocket automatically by using extended Kalman filter (EKF). Section 4 shows the experimental results and discussion. Conclusions are included in Section 5.

2 Process of fast reconstruction

Owing to its enormous size and complicated movement modes, an engineering vehicle is difficult to drive manually under limited field of view. Besides, the human operator must have high capability of hand-eye coordination. For this reason, manual operation is not universal under the occasions of complicated or dangerous environments, especially with the requirements of high accuracy and security.

2.1 Platform of engineering vehicle

The platform of the engineering vehicle used in this paper is a huge flat-bed truck, which uses a diesel engine to drive the hydraulic transmission system for transporting heavy goods. Fig. 1 shows the prototype of the vehicle, which has several wheels under both sides of the chassis. It has the function of multi-wheel independent driving and each wheel has its own rotating shaft [11]. This structure leads to several motion and steering patterns including straight movement, oblique movement, turning around etc. Since the hydraulic transmission system has poor performance of synchronisation, the pose of the chassis has a subtle distinction with the one of the upper platform, especially when the vehicle turns around. The upper platform on the chassis of the vehicle could be elevated upwards or downwards so as to make the platform horizontal when

Fig. 1 *Image of the engineering vehicle*

carrying heavy cargo. Under the present handy mode, the human operator manipulates the big vehicle in the driving room or operates it with a remote controller in the distance.

The on-vehicle control system is an embedded controller based on a PC104 card, which is extended with a data acquisition card and other peripheral devices to compose a compact integrated computer. The controller decides the movement of the vehicle as a response to the input information from the control panel. The interface of controller area network (CAN) on the vehicle provides the function of data communication with other controllers. The open control architecture of is a prerequisite for the following reconstruction for intelligentisation.

2.2 *Reconstruction for intelligentisation*

To make the engineering vehicle work automatically in different working conditions, a reconstruction process is explored by adding exteroceptive sensor suite and a higher-level controller on the vehicle. The hardware relative to the sensors and the control system is arranged as follows.

2.2.1 Sensor suite: Under the chassis of the engineering vehicle, the wheels of the first and the last rows are driven by hydraulic motors. And the number of pulse of each hydraulic motor could coarsely represent the mileage of each wheel. Besides, a magnetic encoder is fixed on each wheel's rotating shaft. Since the structure of multiple wheels leads to complicated motion modes, and sometimes a few wheels run in idleness, the relative movement of the vehicle could not be calculated easily and reliably by using odometry as is usual for intelligent vehicles. In many cases, the accurate pose of the upper platform is of interest for control. However, there is a small difference between the pose of the upper platform and the one of the chassis. So it is necessary to install exteroceptive sensors on the platform directly.

GPS and vision sensors are widely used on intelligent vehicles. However both of them are subject to working conditions, which result in unstable sensory data. To ensure the environmental adaptability, two-dimensional (2D) laser scanners are used on the engineering vehicle. Two laser scanners are fixed to perceive the surrounding environment and estimate the relative pose of the vehicle. Here, the 2D laser scanners are SICK LMS111 laser range finders [12]. The two sensors are installed on both sides of the mounting frame with different heights and longitudinal distances so as to avoid crosstalk interference between laser beams from two sensors. In addition, a 2-axis inclinometer is already fixed on the upper platform to keep it horizontal. Fig. 2 shows the arrangement of sensors on the vehicle.

2.2.2 Control architecture: The control architecture of the unmanned engineering vehicle is composed of higher-level and lower-

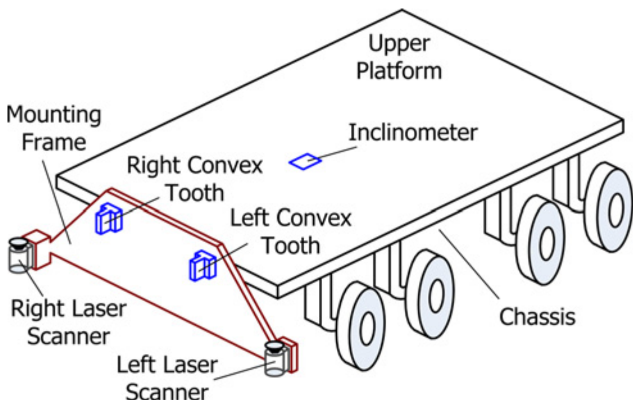

Fig. 2 *Sensors added on the engineering vehicle*

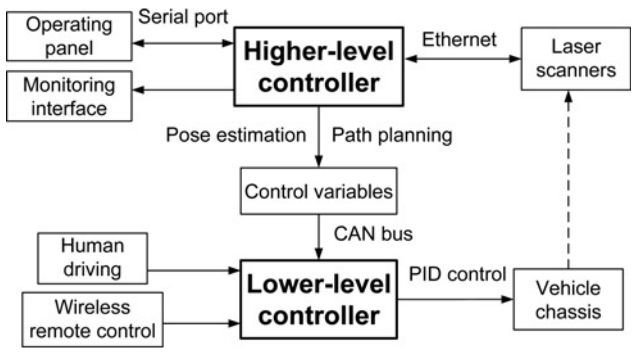

Fig. 3 *Diagram of the closed-loop control system*

level controllers. In the higher-level controller, the sensory data from two laser scanners are sent to an industrial personal computer (PC) by Ethernet. The human machine interface has two parts, that is, the operating panel and the monitoring interface. The industrial PC mainly processes the sensory data and estimates the vehicle pose in real time. Besides, path planning is handled at the same time. Then, the control variables are sent to the lower-level controller, that is, the present on-board controller mentioned in Section 2.1, by CAN bus. In the lower-level controller, the motion mode is selected first and then proportional–integral–derivative (PID) algorithm is used to control the vehicle according to the current and the expected poses. The heading angle and position of the vehicle is regulated so as to move along the planned path continuously. The two-level controllers together with the sensors form a closed-loop system, which is shown in Fig. 3. The monitoring interface is a graphical user interface for displaying data processing and pose estimation, and the operating panel could provide the operator with the vehicle pose and on-site vision information.

3 Application to carrying rocket

3.1 *Background of carrying rocket*

To establish a quick launching system for rockets with small and medium sizes, a half-physical simulation system is built to verify its feasibility and flexibility. In this large-scale system, an engineering vehicle navigation sub-system is set up first to transport the rocket horizontally to the launching site and align with the launcher perpendicularly. Then, the rocket is lifted up vertically on the launcher. Considering that the precise alignment between the rocket and the launcher could avoid using an additional mechanism to regulate the rocket's pose, the accuracy of automatic navigation must be high. According to the given engineering vehicle, it depends mainly on the performance of pose estimation. Although, the traditional process of alignment guided by human operators is difficult under the needs of high accuracy and smoothness.

For the sake of easy perception by laser scanners, the structure of the launcher is designed particularly. The simplified launcher is mainly made up of one big front board, two small boards and cylindrical landmarks on both sides. Fig. 4 shows the detailed structure of the launcher.

3.2 *Localisation of the unmanned engineering vehicle*

When transporting the rocket, the upper platform of the engineering vehicle keeps horizontal. Besides, the launching site could be seemed as an ideal horizontal 2D environment. So the vehicle pose at the kth sampling instance is denoted as the status vector $\boldsymbol{x}(k) = (x_k, y_k, \psi_k)^{\mathrm{T}}$. Here, the first two variables determine the position and ψ_k is the heading angle in the global coordinate frame xOy. An EKF [13] is used to estimate the vehicle's pose relative to the launcher recursively. In each recursion, status prediction and measurement update together form the frame of filtering.

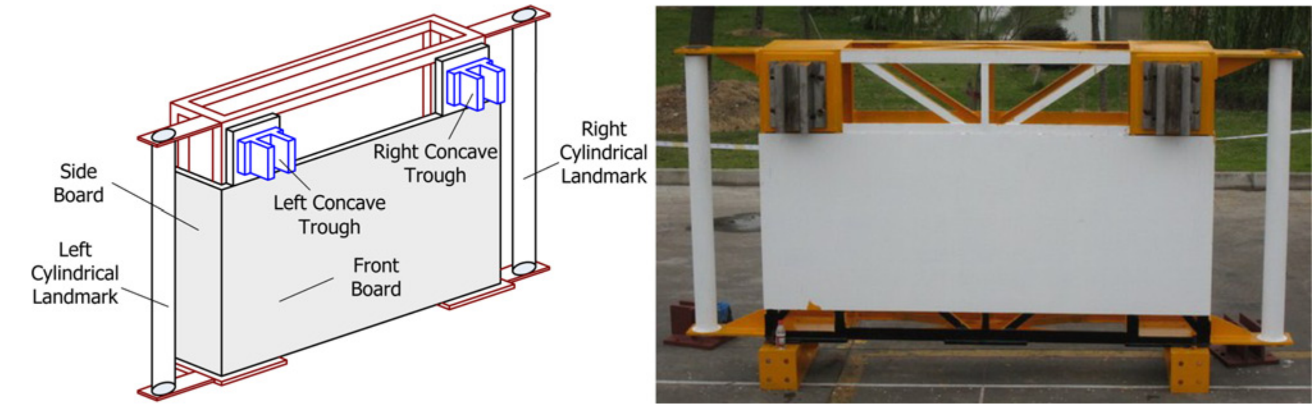

Fig. 4 *Structure of the simplified launcher*

3.2.1 Status prediction: If the vehicle's motion function $\boldsymbol{f}(\cdot)$ is known accurately, the vehicle's new pose at time instance $k+1$ could be represented as

$$\boldsymbol{x}(k+1) = \boldsymbol{f}(\boldsymbol{x}(k), \quad \boldsymbol{u}(k+1), \quad \boldsymbol{w}(k+1)) \tag{1}$$

where $\boldsymbol{u}(k+1)$ and $\boldsymbol{w}(k+1)$ are the control input and the process noise, respectively. In traditional intelligent vehicles, $\boldsymbol{u}(k+1)$ is usually calculated with odometry by using interoceptive sensors.

Taking into account the complicated motion modes and deficient configuration of sensors, the engineering vehicle only uses laser scanners to perceive the change of its position relative to the launcher. Therefore the two laser scanners first detect the line segment corresponding to the front board of the launcher. Then, the two end points and the direction of the line segment could be extracted. The change of the parameters of the line segment in k and $k+1$ time instances is designated to the control input $\boldsymbol{u}(k+1)$ [14]. So the predicted value of $\boldsymbol{x}(k+1)$ and its covariance matrix are

$$\hat{\boldsymbol{x}}^-(k+1) = \hat{\boldsymbol{x}}(k) \oplus \boldsymbol{u}(k+1) \tag{2}$$

$$\boldsymbol{P}^-(k+1) = \boldsymbol{P}(k) + \boldsymbol{Q}(k+1) \tag{3}$$

where the hat ^ above the status vector denotes its estimated value and the additive superscript $^-$ denotes the predicted value. The symbol $\oplus$ represents the compounding operation of two vectors [15]. The covariance matrix of the process noise $\boldsymbol{w}(k+1)$ is denoted as $\boldsymbol{Q}(k+1)$, which is decided by the value of $\boldsymbol{u}(k+1)$. In this navigation system, the vehicle's heading angle keeps small in most cases (e.g. $\psi_k < 5°$). So $\boldsymbol{P}^-(k+1)$ is replaced by the sum of $\boldsymbol{P}(k)$ and $\boldsymbol{Q}(k+1)$ approximately.

3.2.2 Measurement update: In this stage, each laser scanner detects the cylindrical features in the environment and then corrects the vehicle's pose according to the residual of measurement. The relationship between the new measurement vector $\boldsymbol{z}(k+1)$ and the measurement function $\boldsymbol{h}(\cdot)$ is represented as

$$\boldsymbol{z}(k+1) = \boldsymbol{h}(\boldsymbol{x}(k+1), \quad \boldsymbol{m}(j), \quad \boldsymbol{v}(k+1)) \tag{4}$$

where $\boldsymbol{v}(k+1)$ is the measurement noise. And $\boldsymbol{m}(j) = (x_j, y_j)^{\mathrm{T}}$, which means the position of the jth feature in the environmental map corresponding to the current measurement vector $\boldsymbol{z}(k+1)$.

Each cylindrical landmark's centre on both sides of the launcher is first extracted according to laser sensor data and then matched to the landmark map. Providing that the measurement vector $\boldsymbol{z}(k+1) = (z_r, z_\theta)^{\mathrm{T}}$ corresponds to one landmark's centre, it is composed of the distance z_r and the angle z_θ of the landmark relative to the sensor. The predicted measurement vector is

$$\hat{\boldsymbol{z}}(k+1) = \begin{bmatrix} \sqrt{(x_j - \hat{x}_L^-)^2 + (y_j - \hat{y}_L^-)^2} \\ \operatorname{atan}\left(\dfrac{y_j - \hat{y}_L^-}{x_j - \hat{x}_L^-}\right) - \hat{\psi}_{k+1}^- + \pi/2 \end{bmatrix} \tag{5}$$

where the predicted value of one sensor's position is $(\hat{x}_L^-, \hat{y}_L^-)^{\mathrm{T}}$ and $\hat{\psi}_{k+1}^-$ is the predicted heading angle of the vehicle. The difference between the sensory data and the predicted measurement value, that is, the residual of measurement, and its covariance matrix are

$$\boldsymbol{\nu}(k+1) = \boldsymbol{z}(k+1) - \hat{\boldsymbol{z}}(k+1) \tag{6}$$

$$\boldsymbol{S}(k+1) = \nabla \boldsymbol{h}_x \boldsymbol{P}^-(k+1) \nabla \boldsymbol{h}_x^{\mathrm{T}} + \boldsymbol{R}(k+1) \tag{7}$$

where $\nabla \boldsymbol{h}_x$ means the partial derivative of $\boldsymbol{h}(\cdot)$ relative to the vehicle's pose at its predicted value. The covariance matrix $\boldsymbol{R}(k+1)$ is decided by the measurement noise $\boldsymbol{v}(k+1)$ of the sensor.

Now calculate the Kalman gain matrix as

$$\boldsymbol{K}(k+1) = \boldsymbol{P}^-(k+1) \nabla \boldsymbol{h}_x^{\mathrm{T}} \boldsymbol{S}(k+1)^{-1} \tag{8}$$

Then the posterior estimation of the vehicle pose after correction and its covariance matrix are

$$\hat{\boldsymbol{x}}(k+1) = \hat{\boldsymbol{x}}^-(k+1) + \boldsymbol{K}(k+1)\boldsymbol{\nu}(k+1) \tag{9}$$

$$\boldsymbol{P}(k+1) = (\boldsymbol{I} - \boldsymbol{K}(k+1)\nabla \boldsymbol{h}_x)\boldsymbol{P}^-(k+1) \tag{10}$$

where $\boldsymbol{I}$ is an identity matrix.

3.2.3 Laser sensor data processing: In the two recursive stages mentioned above, both the priori and the posteriori estimations depend on the measurement data of the two 2D laser sensors installed on the head of the vehicle. Owing to the complicated environment and the characteristics of detection, each frame of sensory data is constituted by a number of dispersed 2D points in sequence. To find the measurement points corresponding to the boards and the cylinders, data segmentation is used first to divide each frame into several point clusters based on the distances between adjacent points. Then, the isolated and dispersed points are discarded. According to the rest of point clusters, line segment fitting and arc fitting are used to extract the geometric positions corresponding to the landmarks (see Fig. 5). Feature

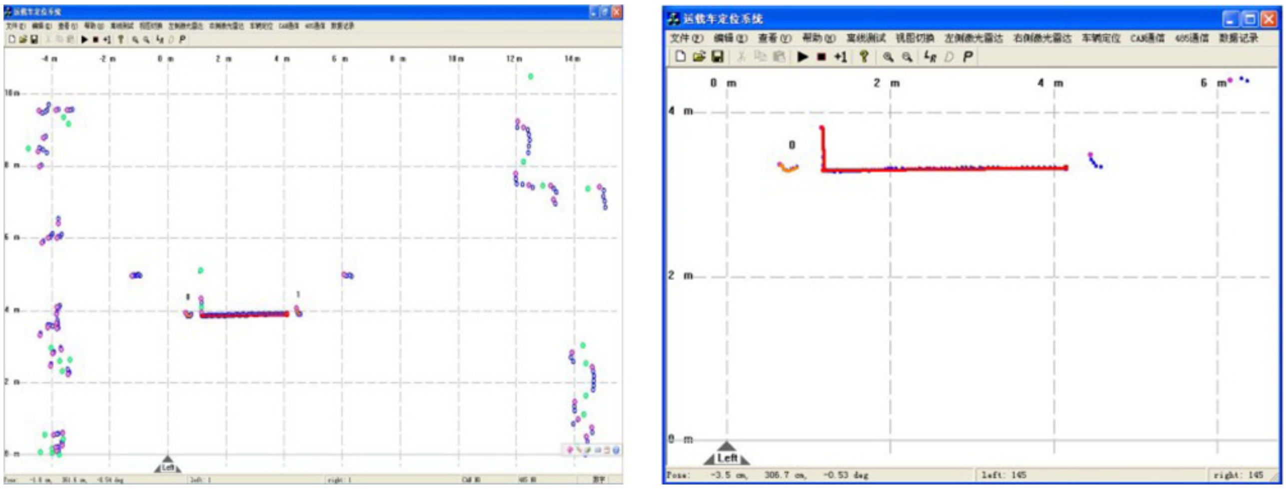

Fig. 5 *Data clustering and feature extraction of one laser sensory frame*

extraction of laser sensory data is used to solve two positioning problems:

(a) *Initial pose estimation*: When the vehicle's initial pose is unknown, the front board and the two side boards on the launcher are detected first. According to the end points of the line segment corresponding to the front board or the corners between the front and the side boards, the position and direction of the front board could be calculated.
(b) *Recursive pose estimation*: When using EKF algorithm to estimate the vehicle's pose in real time, detections of the front board and the cylinders are executed independently (see Sections 3.2.1 and 3.2.2). Since the predicted estimation of the pose is known, a region of interest is used to search the valid measurement points in each sensory frame quickly.

4 Experimental results and discussion

4.1 Experimental platform

The unmanned engineering vehicle after reconstruction is shown in Fig. 6, which is based on a heavy platform vehicle with allowable payload of 100 tons. To test if the vehicle is navigated towards the launcher successfully, two convex teeth on the front of the upper platform and two concave troughs on the launcher are used (see Figs. 2 and 4). The breadth of the gap on each concave trough is 2 cm larger than the one of each convex tooth. The navigation system automatically guides the vehicle towards the launcher until each convex tooth inserts the corresponding concave trough successfully. That means the final alignment error must be in the scope of 1 cm. Besides the accuracy of the lateral position, the vehicle should keep perpendicular with the launcher so that both the two convex teeth insert the concave troughs concurrently.

4.2 Path planning

Before entering the automatic navigation zone, the vehicle is manually guided in front of the launcher at a distance of about 10 m and with a small heading angle. Then, the vehicle approaches the launcher automatically and adjusts the deviation of relative pose to zero gradually. The path planning is divided into several steps:

(a) To decrease the heading angle of the vehicle to zero, the pattern of rear wheel steering is selected so as to have a small change on the position of the vehicle's front end.
(b) If the vehicle deviates from the central axis of the launcher, the pattern of oblique movement is applied until the centre of the vehicle's front end approaches to the central axis.
(c) By selectively using the patterns of straight movement, oblique movement or rear wheel steering, the vehicle closes to the launcher in a straight line approximately. When each convex tooth on the vehicle inserts the corresponding concave trough on the launcher successfully, the vehicle stops moving forward.

Fig. 7 shows the global coordinates xOy, which are fixed on the launcher. Since the two laser sensors are installed at the head of the vehicle, the vehicle coordinates $x_fO_fy_f$ are placed at the midpoint of the two sensors at O_l and O_r. So the uncertainty of pose estimation by using EKF algorithm could propagate slowly. Then, the current

Fig. 6 *Unmanned engineering vehicle after reconstruction*

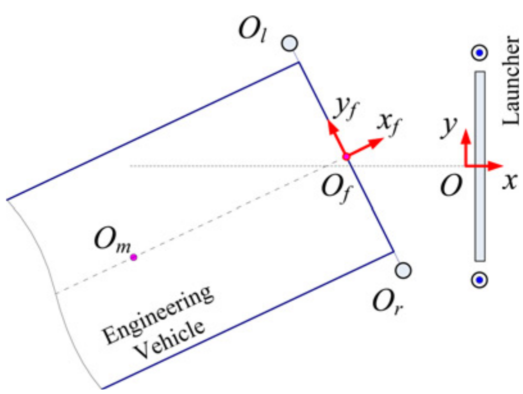

Fig. 7 *Global coordinates and the vehicle coordinates*

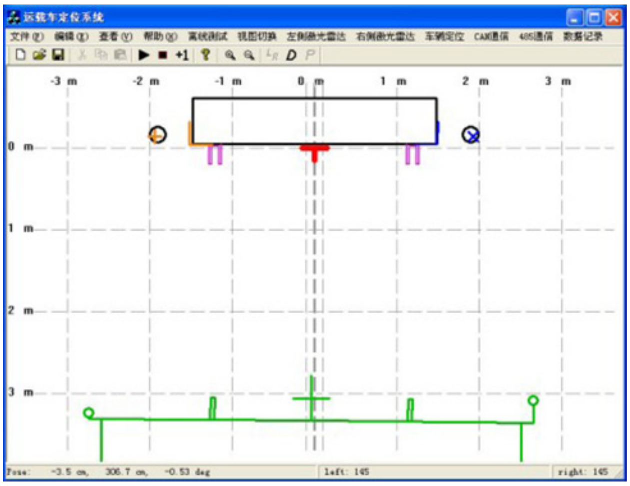

Fig. 8 *Interface of the positioning system*

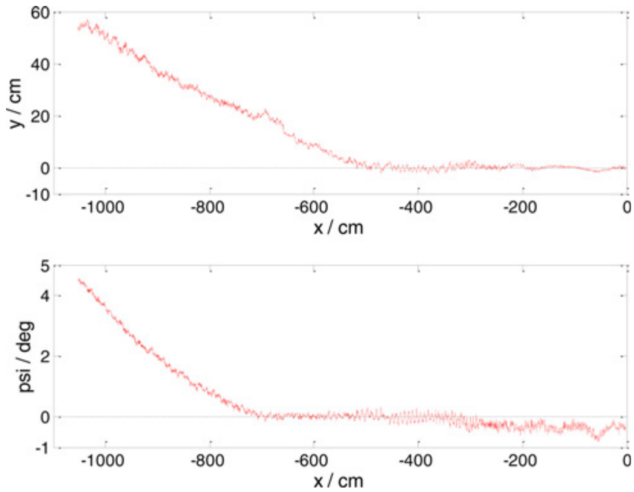

Fig. 9 *Vehicle's trajectory of localisation*

vehicle pose at the point O_f is converted to the pose at the vehicle's geometric centre O_m, which is the basic reference for movement control of lower-level controller. According to the vehicle's pose estimation and path planning, the on-vehicle control system selects the motion patterns and uses PID control algorithm to regulate the vehicle towards the launcher.

4.3 *Experimental results*

The operation interface of the engineering vehicle's positioning system is shown in Fig. 8, which draws the simplified launcher and the vehicle's estimated pose on the top and bottom of the picture, respectively. In the navigation process, the vehicle moves towards the top slowly until the pose alignment is achieved.

The result of localisation and navigation when the vehicle is approaching to the launcher is shown in Fig. 9, which includes each position and heading angle on the trajectory. The result also shows that there are small jumps between adjacent estimated poses. These jumps are probably the result of frequent switchover of control between different motion patterns. So the threshold values governing the motion patterns have to be enlarged, which lead to bigger navigation deviations of the lateral position and the heading angle. The final positioning error includes a lateral error of 0.5 cm and an angular error of 0.4°. It is allowable and the perpendicular alignment of the vehicle to the launcher could be guaranteed. Finally, the two convex teeth on the vehicle insert into the corresponding concave troughs simultaneously. Fig. 10 shows the insertion process from different viewpoints. The vehicle will stop moving forward until the longitudinal distance to the launcher approaches to zero.

In the navigating process, the heading angle of the vehicle is small throughout. Therefore the linearisation error of EKF algorithm has a small effect on the estimation results. Since there are no special sensors added to estimate the vehicle's relative movement at the status prediction step, the localisation results have small jumps between adjacent sampling instances. If the estimated trajectory is smoothed, then the accuracy of navigation could be improved further.

According to the localisation and navigation experiments, the laser sensors added on the vehicle are suitable for detecting geometric features in the environment. The two laser radars arranged on both sides of the vehicle's forehead could decide the accurate pose of the big platform. In addition, the estimated position of the vehicle is selected near the two laser sensors so that the error propagation of the status estimation could be limited as small as possible.

5 Conclusions and future work

This paper presents the fast reconstruction process of an unmanned engineering vehicle by adding a higher-level controller and two 2D laser range finders on the moving platform. Then, an EKF is used to localise the engineering vehicle for carrying a small-size rocket towards a launcher accurately. The lateral positioning error for navigation is smaller than 1 cm so that the vehicle could be in alignment with the launcher successfully. This reconstruction provides an option for fast automation of engineering vehicles, which improves

Fig. 10 *Side and top views of the convex teeth inserting into the concave troughs*

the working efficiency and safety. Meanwhile, the CAN and Ethernet communications give the precondition for realising modular design of vehicles and intelligentisation of machinery group.

To make the reconstruction of engineering vehicle widely applied and popularised, our future work will focus on increasing the navigation accuracy and reliability under faster speed. The aim of this research is to realise automated engineering vehicle platoon, which is made up of many small unattached vehicle modules and capable of carrying huge loads intelligently.

6 Acknowledgment

This project was supported by the National Natural Science Foundation of China (grant no. 51205104).

7 References

[1] Buehler M., Iagnemma K., Singh S.: 'The DARPA urban challenge – autonomous vehicles in city traffic', in Siciliano B., Khatib O. (Eds.): 'Springer tracts in advanced robotics' (Springer, 2009), pp. 1–60

[2] Barbeau S.J., Winters P.L., Georggi N.L., Labrador M.A., Perez R.: 'Travel assistance device: utilising global positioning system-enabled mobile phones to aid transit riders with special needs', *IET Intell. Transp. Syst.*, 2010, **4**, (1), pp. 12–23

[3] Wender S., Dietmayer K.: '3D vehicle detection using a laser scanner and a video camera', *IET Intell. Transp. Syst.*, 2008, **2**, (2), pp. 105–112

[4] Zhao H.J., Chiba M., Shibasaki R., Shao X.W., Cui J.S., Zha H.B.: 'A laser-scanner-based approach toward driving safety and traffic data collection', *IEEE Trans. Intell. Transp. Syst.*, 2009, **10**, (3), pp. 534–546

[5] Broggi A., Cerri P., Ghidoni S., Grisleri P., Jung H.J.: 'A new approach to urban pedestrian detection for automatic braking', *IEEE Trans. Intell. Transp. Syst.*, 2009, **10**, (4), pp. 594–605

[6] Zavadskas E.K.: 'Automation and robotics in construction: international research and achievements', *Autom. Constr.*, 2010, **19**, (3), pp. 286–290

[7] Ha Q., Santos M., Nguyen Q., Durant-Whyte H.: 'Robotic excavation in construction automation', *IEEE Robot. Autom. Mag.*, 2002, **9**, (1), pp. 20–28

[8] Yamamoto H., Moteki M., Shao H., *ET AL.*: 'Development of the autonomous hydraulic excavator prototype using 3-D information for motion planning and control'. 2010 IEEE/SICE Int. Symp. System Integration, Sendai, Japan, 2010, pp. 49–54

[9] Marshall J.A., Murphy P.F., Daneshmend L.K.: 'Toward autonomous excavation of fragmented rock: full-scale experiments', *IEEE Trans. Autom. Sci. Eng.*, 2008, **5**, (3), pp. 562–566

[10] Lu M., Chen W., Shen X.S., Lam H.C., Liu J.Y.: 'Positioning and tracking construction vehicles in highly dense urban areas and building construction sites', *Autom. Constr.*, 2007, **16**, (5), pp. 647–656

[11] Li Y.H., Yang L.M., Zhang Z.H.: 'Development of power flat transporter for conveying heavy frame components in shipbuilding', *Ship Eng.*, 2005, **27**, (1), pp. 67–72 (in Chinese)

[12] SICK AG.: 'LMS100/111/120 laser measurement systems', 2008

[13] Welch G., Bishop G.: 'An introduction to the Kalman filter'. TR95-041, ACM, USA, 2001

[14] Qian J., Zeng Y.S., Wang S.W.: 'An engineering vehicle positioning system for carrying rocket using extended Kalman filter'. Third Int. Conf. Mechanical and Electronics Engineering, Hefei, China, 2011, (3), pp. 422–426

[15] Smith R., Self M., Cheeseman P.: 'A stochastic map for uncertain spatial relationships'. Fourth Int. Symp. Robotics Research, Cambridge, USA, 1987, pp. 467–474